

Experimental investigation of Heat and mass transfer in a LiBr-H₂O solution falling film absorber on horizontal tubes: Comprehensive effects of tube types and surfactants

Huan Zhang^{a, b}, Dazhen Yin^a, Shijun You^{a, b}, Wandong Zheng^{a, b, *}, Shen Wei^c

^a *School of Environmental Science and Engineering, Tianjin University, Tianjin, 300350, China*

^b *Key Laboratory of Efficient Utilization of Low and Medium Grade Energy, MOE, Tianjin University, Tianjin 300350, China*

^c *The Bartlett School of Construction and Project Management, University College London (UCL), 1-19 Torrington Place, London WC1E 7HB, United Kingdom*

** Corresponding Author: Tel. / Fax: +86 22 2789 2626. E-Mail address: wdzheng@tju.edu.cn*

Abstract

This paper studied the effects of various surface geometries and surfactants on the LiBr-H₂O solution falling film absorption, and the heat and mass transfer during the absorption process. Three different tubes (plain tube, floral tube and floral finned tube) were tested for the LiBr-H₂O solution with two different surfactants (2-Ethyl-1-hexanol and 1-Octanol). The results indicate that the heat and mass transfer coefficients of each tube gradually decrease with solution falling down the tube bundle. It is also showed that the effect of surfactant on heat and mass transfer is obviously greater than that of tube surface geometry. Furthermore, with 2-Ethyl-1-hexanol as the surfactant, the heat and mass transfer can be improved by 400% and 350%, respectively. The results of comparative study show that the heat and mass transfer performance of floral tubes with 2-Ethyl-1-hexanol is more stable and reliable than others.

Keywords:

Heat and mass transfer coefficients, LiBr-H₂O solution, falling film absorption, tube types, surfactants

Nomenclature	
K	heat transfer coefficient (W/(m ² ·K))
T	temperature (°C)
Q	thermal load (kW)
c	specific heat capacity (kJ/(kg·K))
\dot{m}	mass flow rate (kg/s)
h	enthalpy (kJ/kg)
F	area (m ²)
F'	surface area per meter tube length (m ² /m)
n	tube number (n)
d	tube diameter (m)
r	tube radius (m)
L	tube length (m)
u	velocity of flow (m/s)
ν	kinematic viscosity (m ² /s)
V	volume flow (m ³ /h)
P	pressure (kPa)
Nu	Nusselt number
Re	Reynolds number
Pr	Prandtl number
Subscripts	
$total$	total absorber
ln	logarithm
out	outlet
in	inlet
o	outside
i	inside
s	solution

<i>w</i>	water
<i>copper</i>	copper
<i>film</i>	falling film
<i>absorbed</i>	absorbed
<i>v</i>	vapor
Greeks	
β	mass transfer coefficient (g/(m ² ·s))
ρ	density (kg/m ³)
ξ	solution mass fraction (wt%)
$\Delta\xi_{ln}$	logarithmic mean mass fraction difference (%)
ξ'	equilibrium mass fraction of LiBr-H ₂ O solution (%)
Γ	spray density (kg/(m·s))
λ	thermal conductivity (W/(m·K))

1 Introduction

With the increasing demands of energy recovery, a growing number of scholars have conducted studies on absorption refrigeration, whose development is of practical values in reality. Absorption refrigeration is positively encouraged due to its economy and energy saving property by using low-grade energy as driving energy, such as industrial waste heat, geothermal energy. At the same time, absorption heat pump is also harmless to the environment by using environment-friendly working pair, such as LiBr-H₂O solution and ammonia-H₂O solution. The energy and economic efficiency of LiBr absorption heat pump system is determined by the heat and mass transfer performance of LiBr-H₂O solution falling film on the horizontal tube bundle. Therefore, the research on heat and mass transfer of absorber has aroused much interests [1-3].

Rogdakis et al. [1] developed a model of the vapor absorption of LiBr-H₂O

solution, and the effect of absorption heat variation on the temperature field is discussed in detail. Kyung et al. [2] built models to simulate the falling film absorption of LiBr-H₂O solution on horizontal tubes, and the flow was divided into three regimes: falling film in contact with the tube; drop formation at the bottom of the tube; and drop fall between the tubes. Zhao et al. [3] discussed the subcooled falling film heat transfer on a horizontal tube, and analyzed the effects of film flow rate, heat flux, inlet liquid temperature, tube diameter and liquid distributor height. Triché et al. [4] analyzed the absorption process in a falling film absorber by experimental and numerical methods, and the results showed that mass transfers are controlled by the falling film mass transfer resistance. Álvarez and Bourouis [5] investigated the heat and mass transfer performance in a horizontal tube falling film absorber, and the working pair were aqueous (lithium, potassium, sodium) nitrate solution. The absorber efficiency of this working pair was similar to that of water/LiBr with additives. Li et al. [6] studied the heat and mass transfer performance of falling film absorption by using LiCl solution. The effect of falling film absorber using different solutions was compared, and they found that heat and mass transfer coefficients were related with each other.

It is widely recognized that the heat and mass transfer in the absorption process can be enhanced remarkably by two methods: one is to use high efficiency heat transfer tubes; the other is to add surfactant to the solution [7].

Plain tubes are widely used as heat transfer tubes in absorbers. In order to improve the heat transfer performance and miniaturization of the absorber, heat transfer tubes with various structures have been proposed [8]. Kim and Kang [9] proposed a novel

hydrophilic surface treatment method which uses plasma. The experimental results showed that the tube with high wettability demonstrated a more excellent heat transfer performance compared with the untreated tube. Compared with the non-hydrophilic surface tube, the film flowing on the hydrophilic surface tube had smaller thickness and greater heat transfer area. The research results showed that the heat transfer performance was affected by wetted area on falling-film heat exchanger [10]. When the liquid dropped onto the surface, the water could rapidly wet the surface with a low contact angle. Zheng and Ma [10] used chemical etching method to obtain the superhydrophilic surfaces, the contact angle of which was close to 0° , and the superhydrophilic tubes had a high heat transfer coefficient at low flow rates. Arroiabe et al. [11] analyzed the influence of the contact angle on the wettability of horizontal-tube falling films, and found that the contact angle had great influence on the flow hydrodynamics, flow mode and wetted area. Lee et al. [12] tested heat transfer performance of two different heat transfer tubes (plain and porous-layer coated). Due to the higher wetted rate and heat transfer coefficient, the heat transfer rate of the porous-layer coated tubes is 2 times higher than that of the plain tube.

Adding surfactant to solution is also an effective method to improve the heat and mass transfer performance [13]. Bourne and Eisberg firstly discovered the positive effect of surfactants on heat and mass transfer of absorption refrigeration. Yoon et al. [14] were concerned with the heat transfer enhancement by surfactants and different heat transfer tubes. The results indicated that the hydrophilic tube had the highest heat transfer coefficient and the heat transfer coefficients were increased by 30-90% for all

the tubes with the application of surfactants Sun et al. [15] experimentally studied the effects of operation parameters on mass transfer, and the results indicated that the strong mass transfer enhancement occurred with 2EH (2-ethyl-1-hexanol) of 90 ppm in LiBr-H₂O solution.

The effect of Marangoni convection was involved in many recent studies, which could enhance the heat and mass transfer. Adding a small amount of surfactant to the LiBr-H₂O solution can change the surface tension characteristics of the solution. Kim and Ferreira [16] investigated the effects of surfactant and surface geometry on LiBr-H₂O solution falling films on vertical plates. Marangoni convection was observed in falling film of LiBr-H₂O solution, which resulted in significant enhancement of heat and mass transfer by more than two times through the application of 2-ethyl-1-hexanol. Daiguji [17] investigated the Marangoni effect based on the salting out effect. By LiBr absorption experiments with surfactants, Kulankara [18] proposed that the surfactant in vapor affects the surface tension of LiBr-H₂O solution. Giannetti [19] built numerical model to study the effects of Marangoni convection. Marangoni cell is formed by the coupling of shear stress, surface tension and pressure gradients, and the Marangoni convection affects the heat and mass transfer process of the absorptive mixtures.

This paper is to improve the heat and mass transfer process of falling film absorption with different enhancement methods (with surfactant and different tube surface geometry). The effects of two surfactants (2-Ethyl-1-hexanol and 1-Octanol) and three heat transfer tubes (plain tube, floral tube and floral finned tube) are investigated. The variation of heat and mass transfer coefficients with different solution

spray density, surfactant concentrations and tube types are studied. Comparative studies are conducted to explore the most available and effective way to improve the heat and mass transfer performance.

2. Experimental setup and conditions

2.1 Experimental setup

An experimental setup was established to research the heat and mass transfer performance of absorber with different tubes and surfactants. The schematic diagram of the experimental setup is shown in Fig. 1, which is composed of five parts: solution generation and absorption device, solution heating system, cooling water system, vacuum and sampling system and data acquisition system.

The solution generation and absorption device are the main part of the whole experimental device. These horizontal tube bundles are made up of 14 horizontally arranged copper tubes. The effective length of the horizontal copper tube is 0.5 m with the tube spacing of 16mm. In order to ensure the air tightness of the system, the copper tube is closely connected with the absorber. The cooling water flows in the horizontal tubes. The experimental set of copper tubes consists of three types, including plain tube, floral tube and floral finned tube. In order to observe the absorption process of the falling film, five sight glasses are installed on the absorber. The dilute solution that has absorbed vapor is concentrated at the bottom of the absorber. After the liquid reaches a certain height, solution will flow back to the generator through solution reflux tube.

In the generator, the heat water tubes are immersed into the LiBr-H₂O solution.

The vapor generated by the generator can enter the absorber through vapor rising tube. The concentrated solution heated in generator is transported to the absorber through canned-motor pump. The flowmeter is mounted on the tube to measure the solution flow rate.

The solution heating system consists of electric heater, hot water tank, hot water circulating pump and hot water tube. The hot water temperature is monitored with Pt thermocouples and controlled by the temperature controller by adjusting the temperature signals from the concentrated solution tank.

The cooling water system is composed of cooling water tank, cooling water pump, and flowmeter. The inlet temperature of cooling water is controlled by mixing cold water with outlet water to maintain the cooling water temperature at the required level.

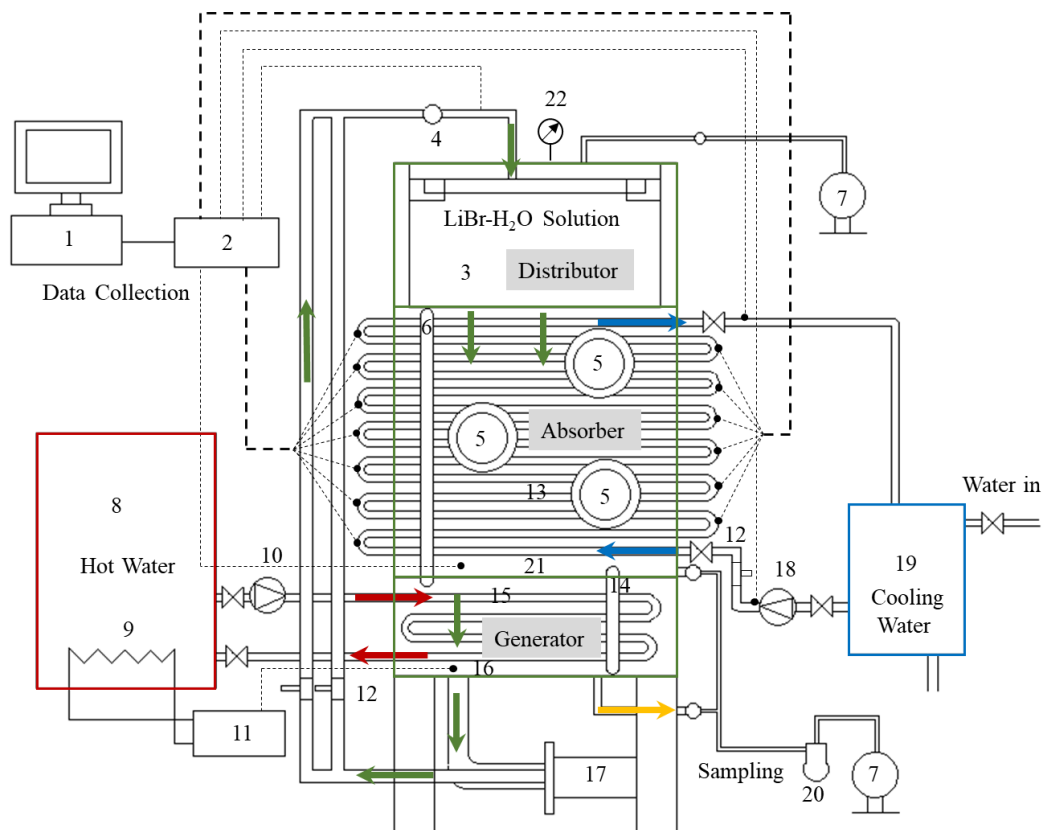
The vacuum and sampling system consist of vacuum tubes, vacuum pump, solution sampling bottle and vacuum valve. Due to the strong corrosiveness of LiBr-H₂O solution to metal, it is important to ensure the experimental setup at vacuum condition. At the same time, the solution sampling bottle collects the solution, and then its mass fraction can be analyzed.

The distribution of testing points is illustrated in Fig.1. The temperatures are measured by copper-constantan thermocouples with the accuracy of ± 0.2 °C. Besides, Turbine flowmeters are used to monitor the volume flow rate of LiBr-H₂O solution with the accuracy of $\pm 0.5\%$. The thermocouples are embedded to measure the temperature continuously and the data are collected by the data collector. The monitored data is collected by the acquisition system. The instrument accuracy is listed in Table 1. The

uncertainty of heat transfer coefficient and the mass transfer coefficient is calculated to be about $\pm 5.8\%$ and $\pm 4.5\%$, respectively.

Table1 Instrumentation accuracy and specifications.

No.	Instrument	Parameter	Uncertainty
1	Canned motor pump	5m; 4m ³ /h; 400W; 3000rpm	-
2	Cooling/hot water pump	8m; 0.5 m ³ /h; 90W	-
3	Vacuum pump	3.6 m ³ /h; 180w; 1400rpm	-
4	Flowmeter	0.04-0.17m ³ /h	$\pm 0.5\%$
5	T-type copper-constantan thermocouple	0-400°C	$\pm 0.2\text{ }^{\circ}\text{C}$
6	Pt100 temperature sensor	-200-850°C	$\pm 0.1 + 0.0017 t \text{ }^{\circ}\text{C}$
7	Pressure gauge	0-0.1mpa	$\pm 1.6\%$
8	Balance	0-500g	0.001g



1-computer 2-data collector 3- Liquid distributor 4- Vacuum valve 5- Sight glass 6- Vapor rising tube 7- Vacuum pump 8- Hot water tank 9- Electric heater 10- Hot water circulating pump 11-

temperature controller 12- Flowmeter 13- Horizontal tube bundle 14- Solution reflux tube 15- Hot water tube 16- Solution generator 17- canned-motor pump 18- Cooling water pump 19- Cooling water tank 20- Solution sampling bottle 21- Solution absorber 22- Pressure gauge

Fig. 1. Schematic of experimental setup for horizontal falling film absorber.



Fig. 2 Photograph of the experimental setup.

2.2 Experimental condition




Experimental conditions are shown in Table 2. The mass fraction of LiBr-H₂O solution in this experiment is 56%. The inlet temperature of LiBr-H₂O solution is controlled at 60 °C to maintain high absorption pressure. The cooling water temperature is 32 °C, and the volume flow rate is 400 L/h. The inlet temperature and volume flow rate of cooling water refer to the actual operation condition of absorption chiller.

Table 2 Experimental conditions.

Items	Parameters	Conditions
Inlet solution	Mass fraction [wt%]	56%
	Temperature [°C]	60
	Spray density [kg/(m·s)]	0.036, 0.054, 0.072, 0.09, 0.11
Cooling water	Inlet temperature [°C]	32
	Flow rate [L/h]	400
Surfactant	2-Ethyl-1-hexanol [ppm]	20, 40, 80, 160, 320
	1-Octanol [ppm]	20, 40, 80, 160, 320

In this study, the plain tube, floral tube and floral finned tube are introduced to improve the heat and mass transfer of the LiBr-H₂O absorber. The parameters of the three tubes are shown in Table 3. The grooves on the surface of floral tube are beneficial to the wetting of tube surface, and the fin promotes the internal disturbance of liquid film. The floral tube and floral finned tube have a great application prospect for their advantage of strengthening heat and mass transfer.

Table 3 Experimental tube parameters.

Type	Outline	Dimension parameter
Plain tube		$d_o=16\text{mm}$ $d_i=14.8\text{mm}$ $F'=0.05024\text{m}^2/\text{m}$
Floral tube		$d_o=15\text{mm}$ $d_i=14.24\text{mm}$ Arc number 11, Arc height 0.5mm $F'=0.05109\text{m}^2/\text{m}$
Floral finned tube		$d_o=15\text{mm}$ $d_i=14.24\text{mm}$ Arc number 11, Arc height 0.5mm Fin height 0.5 mm, fin pitch 26/inch $F'=0.05671\text{m}^2/\text{m}$

The flow rates of LiBr-H₂O solution are controlled by adjusting the canned-motor pump to be 0.12m³/h, 0.1m³/h, 0.08m³/h, 0.06m³/h and 0.04m³/h. Based on the inlet density and tube length, the solution spray density is controlled to be 0.036 kg/(m·s),

0.054 kg/(m·s), 0.072 kg/(m·s), 0.09 kg/(m·s) and 0.11 kg/(m·s). The falling film flow modes from droplet flow to jet flow can be obtained in this spray density range.

The surfactants (2-Ethyl-1-hexanol and 1-Octanol) are used in five different mass fractions of 20 ppm, 40 ppm, 80 ppm, 160 ppm and 320 ppm. It is experimentally demonstrated that the heat and mass transfer coefficients will reach the maximum, and there is significant variation as the surfactant mass fraction exceeds 320 ppm [7].

3. Analysis of measured data

3.1 Temperature and mass fraction of solution on a single tube

When the temperature and mass fraction of inlet and outlet solutions are measured, the heat and mass transfer coefficients of the whole absorber can be calculated. The heat and mass transfer coefficients of each tube are concerned in the designing, but it is hard to measure the temperature and mass fraction of LiBr-H₂O solution for each tube, so an estimation method is adopted to calculate the coefficients of the horizontal tube. The amount of heat absorbed by cooling water in each tube is proportional to the amount of vapor absorbed on the tube surface. By measuring the total vapor absorption and the inlet and outlet temperature of each cooling water tube, the solution temperature and mass fraction at the outlet of each tube can be calculated, and then the heat transfer and mass transfer coefficients of each tube can be obtained.

For the j-th tube in horizontal tube bundle, the energy balance equation can be expressed as:

$$\dot{m}_{s,in,j} \cdot h_s(T_{s,in,j}, \xi_{s,in,j}) + \dot{m}_{v,j} h_v \cdot (T_{s,pool}, P_v) - \dot{m}_w \cdot c_w (T_{w,out,j} - T_{w,in,j}) -$$

$$\dot{m}_{s,out,j} \cdot h_s(T_{s,out,j}, \xi_{s,out,j}) = 0 \quad (1)$$

The vapor temperature is equal to the solution temperature in the generator. Vapor absorption pressure is obtained by the state equation of LiBr-H₂O:

$$P_v = P(\xi_{s,pool}, T_{s,pool}) \quad (2)$$

In the j-th tube, the mass balance equation of LiBr is:

$$\dot{m}_{s,out,j} \cdot \xi_{s,out,j} = (\dot{m}_{s,in,j} + \dot{m}_{v,j}) \cdot \xi_{s,out,j} = \dot{m}_{s,in,j} \cdot \xi_{s,in,j} \quad (3)$$

Assuming that the amount of absorbed vapor is proportional to the heat flux from each tube, the amount of absorbed vapor and the outlet solution mass fraction can be derived from the temperature difference of cooling water in each tube. The following assumptions are made during the calculation: 1) The thermal property of the solution is constant. 2) The transfer coefficient of each tube is considered to be uniformly contributed. 3) The temperature and density of the solution is considered to be uniformly contributed.

According to the energy balance equation, the outlet solution temperature of each tube can be obtained.

$$\dot{m}_{v,j} = \frac{Q_j}{Q_{total}} \cdot \dot{m}_{v,total} = \frac{\dot{m}_w c_w (T_{w,out,j} - T_{w,in,j}) \dot{m}_{v,total}}{\dot{m}_w c_w (T_{w,out} - T_{w,in})} \quad (4)$$

$$\dot{m}_{v,total} = \frac{\dot{m}_{s,in} (\xi_{s,in} - \xi_{s,out})}{\xi_{s,out}} \quad (5)$$

By Eq. (1) - (5), the solution enthalpy and outlet mass fraction of each tube can be obtained. The temperature and mass fraction of outlet solution on the first tube can be calculated by that of inlet solution. The solution outlet parameters of the former tube are the inlet parameters of the latter tube, so the solution inlet and outlet parameters of each tube in tube bundle can be obtained iteratively. The absolute deviation between

the calculated and measured outlet temperature of the last tube is about 1.5 °C, and the relative error between the absolute deviation and the final solution outlet temperature is less than 3%.

3.2 The heat transfer coefficient

The total heat transfer coefficient of absorber is calculated as follows:

$$K_{total} = \frac{Q_{total}}{F \cdot \Delta T_{ln}} \quad (6)$$

In order to calculate heat transfer coefficient, ΔT_{ln} needs to be determined firstly. The LMTD (Logarithmic Mean Temperature Difference) is calculated using the temperature of solution equilibrium and cooling water temperature. The experiment adopts copper-constantan thermocouple as the sensor to collect temperature signal. The ΔT_{ln} of absorber is defined as:

$$\Delta T_{ln} = \frac{(T_{s,in} - T_{w,out}) - (T_{s,out} - T_{w,in})}{\ln \frac{T_{s,in} - T_{w,out}}{T_{s,out} - T_{w,in}}} \quad (7)$$

The total heat flux is based on the inlet and outlet temperatures and mass flow rates of cooling water. The Q_{total} is calculated by:

$$Q_{total} = c_w \cdot \dot{m}_w \cdot (T_{w,out} - T_{w,in}) \quad (8)$$

The total tube bundle area (F) is the sum of 14 tube bundles surface area.

$$F = n \cdot F' \cdot L \quad (9)$$

By substituting Eq. (7), (8) and (9) into Eq. (6), K_{total} is obtained. Substituting K_{total} into Eq. (10), the interface heat transfer coefficient K_{film} can be yielded.

$$\frac{1}{K_{total}} = \frac{r_o}{K_w \cdot r_i} + \frac{r_o \cdot \ln(r_o/r_i)}{\lambda_{copper}} + \frac{1}{K_{film}} \quad (10)$$

The heat transfer coefficient of cooling water can be calculated according to the

Dittus-Boelter equation [22]:

$$K_w = Nu_w \cdot \frac{\lambda_w}{d_i} = 0.023 \cdot Re_w^{0.8} \cdot Pr_w^{0.4} \cdot \frac{\lambda_w}{d_i} \quad (11)$$

The Reynolds number (Re_w) and Prandtl number (Pr_w) of cooling water in Eq. (11) can be defined by:

$$Re_w = \frac{d_i \cdot u_w}{\nu_w} \quad (12)$$

$$Pr_w = \frac{\nu_w}{\alpha_w} \quad (13)$$

3.3 The mass transfer coefficient

Miler [20] proposed the mass transfer coefficient calculation equation, and β_{total} can be identified as:

$$\beta_{total} = \frac{\dot{m}_v \cdot total}{F \Delta \xi_{ln}} \quad (14)$$

$$\Delta \xi_{ln} = \frac{[\xi_{s,in} - \xi'_{s,in}(P_v, T_{s,in})] - [\xi_{s,out} - \xi'_{s,out}(P_v, T_{s,out})]}{\ln \frac{\xi_{s,in} - \xi'_{s,in}(P_v, T_{s,in})}{\xi_{s,out} - \xi'_{s,out}(P_v, T_{s,out})}} \quad (15)$$

Under ideal conditions, the inlet and outlet temperatures of balanced solution $T_{w,in}$ and $T_{w,out}$ are less than the actual ones, so $\xi_{s,in} > \xi'_{s,in}$, $\xi_{s,out} > \xi'_{s,out}$, and the logarithm can be calculated. But However, the outlet solution temperature will rise after adding surfactants when absorption heat cannot be taken away by cooling water immediately. It results in $\xi_{s,out} < \xi'_{s,out}$, and the logarithm in Eq. (15) cannot be solved. To avoid this situation, Francés [21] modified $\Delta \xi_{ln}$. The mass transfer is coupled to the external conditions, so Francés have employed Eq. (16) instead, which refers to the equilibrium mass fraction at the vapor pressure but at the cooling water temperature.

$$\Delta \xi_{ln} = \frac{[\xi_{s,in} - \xi'_{s,in}(P_v, T_{w,out})] - [\xi_{s,out} - \xi'_{s,out}(P_v, T_{w,in})]}{\ln \frac{\xi_{s,in} - \xi'_{s,in}(P_v, T_{w,out})}{\xi_{s,out} - \xi'_{s,out}(P_v, T_{w,in})}} \quad (16)$$

The mass conservation of LiBr is:

$$\dot{m}_{s,in} \cdot \xi_{s,in} = (\dot{m}_{s,in} + \dot{m}_{v,total}) \cdot \xi_{s,out} \quad (17)$$

The vapor absorption quantity is calculated as follows:

$$\dot{m}_{v,total} = \frac{\dot{m}_{s,in} \cdot (\xi_{s,in} - \xi_{s,out})}{\xi_{s,out}} \quad (18)$$

$$\dot{m}_{s,in} = V_{s,in} \cdot \rho_s / 3600 \quad (19)$$

4. Results and discussion

4.1 Heat and mass transfer on the tube bundle

The experiments of LiBr-H₂O solution falling film absorption were done with and without surfactants. Fig. 3 shows the heat and mass transfer coefficients for each tube without surfactant. The solution spray density is 0.036 kg/(m·s). As solution flows down the tubes, vapor is absorbed by the solution continuously, and solution mass fraction decreases. Therefore, the mass transfer coefficients of three types of tubes decrease as the tube number increases. At the same time, it is seen that the mass transfer coefficient of floral finned tube is the largest, followed by that of floral tube and plain tube. It is because the mass transfer coefficient is related to the wetting rate of tube surface. Through the sight glass, it can be seen that the falling film solution merges into several relatively large solution flows as it flows downward along tube bundles. The solution increases the thickness of liquid film and reduces the wetting rate of tube surface, so that the decline of mass transfer coefficient of plain tube is faster than the other type of tubes. For floral tube, the grooves on tube surface guide the solution flowing in the axial direction and the spreading area of solution on the tube surface is

increased, thus it has higher mass transfer coefficient than plain tube. Similarly, the grooves on the surface of floral finned tube can also guide the spreading of solution. Although fins restrain the spreading of solution at low flow rate, those also cause the mixing flow of liquid film on tube surface and promote the mixing of solution, thus improving the heat and mass transfer efficiency. As illustrated in Fig. 3, floral finned tube is superior to floral tube in both heat and mass transfer coefficients.

Although the mass transfer coefficient of plain tube is the lowest, it has the highest heat transfer coefficient in initial phase (Tube 1-8). This phenomenon is caused by the coupling effects between heat and mass transfer processes. For plain tube, the heat and mass transfer coefficients decrease rapidly after the 10th tube. If plain tube is used in absorber, the tube number should be controlled in vertical direction, while in horizontal direction the tube number is considered to be increased to promote the heat and mass transfer performance. The floral tube has high wetting rate, and its heat and mass transfer performance show little variation as the tube number increasing. For floral finned tube, the wetting effect of tube surface is not so good as that of floral tube. However, due to the disturbance of fins, the mass transfer coefficient of floral finned tube is the highest. Comprehensively considering the heat and mass transfer coefficient, floral finned tube has the best effect.

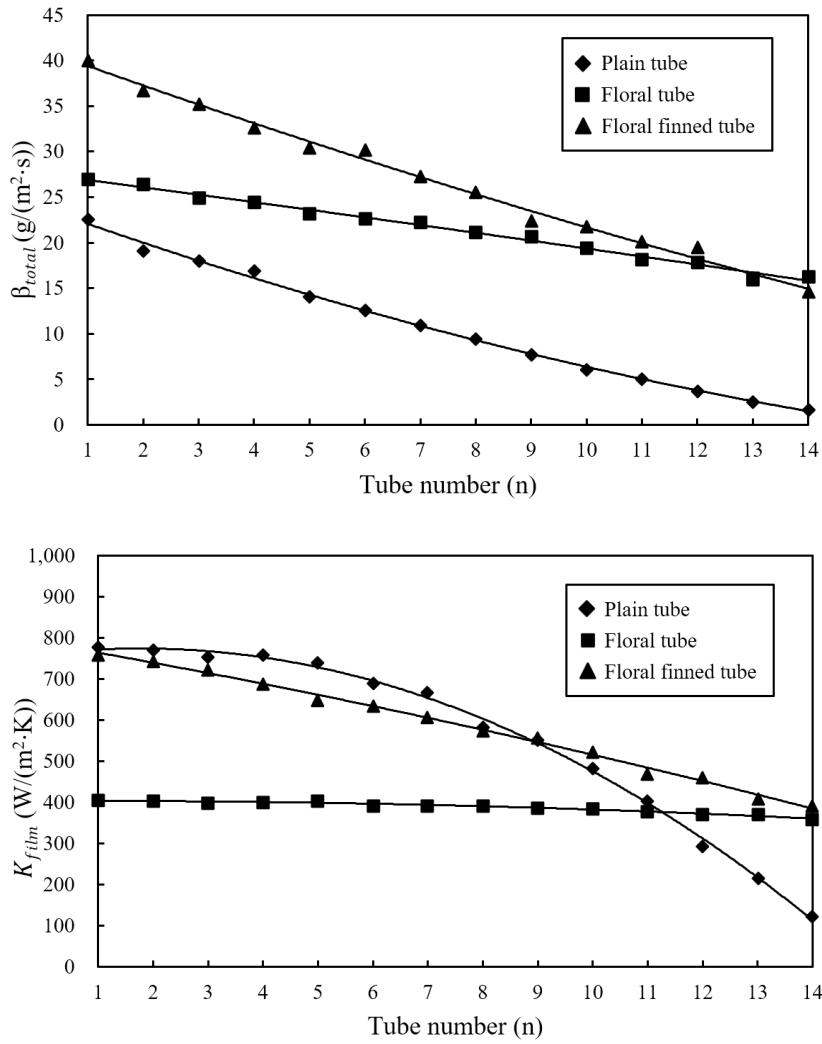


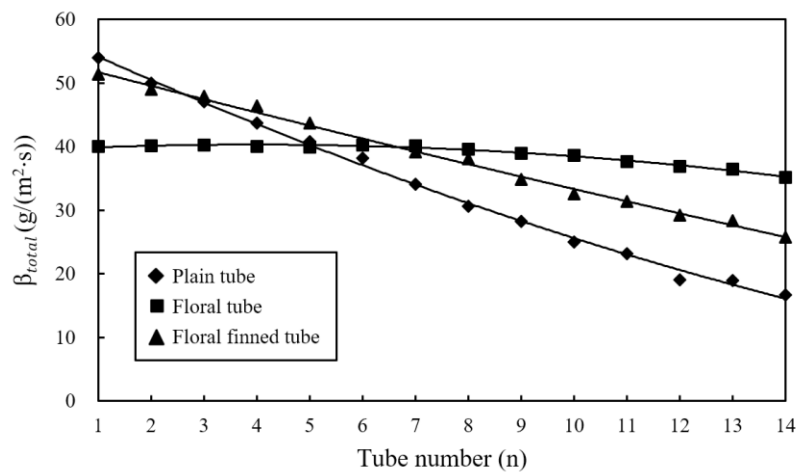
Fig. 3 Heat and mass transfer coefficients of each tube row in horizontal tube bundle ($\Gamma = 0.036 \text{ kg}/(\text{m}\cdot\text{s})$, without surfactant).

As shown in Fig. 4, the heat and mass transfer performance of each row of tubes have been significantly improved with the application of surfactant. As surfactant has the effect of promoting the Marangoni convection, the wetting rate of solution on tube surface is increased. Therefore, the heat and mass transfer curves of the three types of tubes are relatively higher.

The mass transfer coefficient of floral finned tube in initial phase (Tube 1-4) is very close to that of plain tube, and higher than that of the floral tube. However, at the

bottom of tubes, due to the confluence of solution, the mass transfer coefficient of plain tube decreases rapidly, followed by floral finned tube and floral tube.

In terms of heat transfer coefficient, the change of floral tube is the smallest. The heat transfer coefficient of plain tube is always high, but the decline rate is also the largest. At the top row of tubes, the heat transfer coefficient of floral finned tube is lower than that of plain tube, but larger than that of floral tube. The downward trend of floral finned tube is smoother than plain tube. In the bottom of tubes, the heat transfer coefficient of plain tube and floral finned tube is lower than floral tube, it can be attributed to the small amount of vapor absorption, and the reduction of heat transfer capacity. Under the effect of surfactant, the heat and mass transfer coefficients on floral tubes are comparatively uniform. Surfactant has the most obvious enhancement effect on plain tube, and the growth of heat and mass transfer coefficients is the most noticeable.



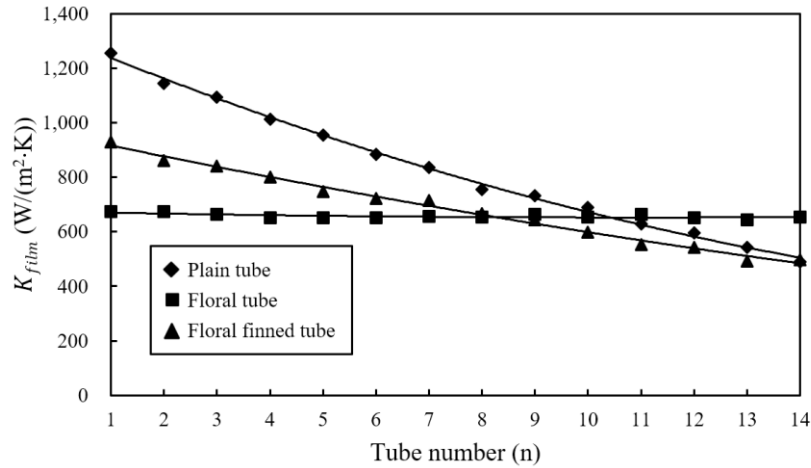


Fig. 4 Heat and mass transfer coefficient on each row of tube bundles ($\Gamma = 0.036$ kg/(m·s), 40 ppm 2-Ethyl-1-hexanol).

4.2 Comparison of Influencing Factors on Heat and Mass Transfer

Fig. 5 shows the mass transfer coefficient under different solution spray density on three types of tubes. As shown in the figure, with the rise of solution spray density, the variation of mass transfer coefficients on different tube types is different. For the plain tube, the mass transfer coefficient grows slowly with the increase of the solution spray density when there is no surfactant. The wetting rate of tube surface increases with the rise of solution flow rate, so the mass transfer coefficient increases. As to the floral tube and floral finned tube, the mass transfer coefficient decreases and tendency is getting smaller with the increase of solution flow rate. It can be attributed to the improvement of wetting rate of the floral tube and floral finned tube, and the decrease of contacting time between the liquid film on tube surface and the vapor with the increase of solution spray density.

As shown in Fig. 5, the floral finned tube has the best mass transfer performance

when there is no surfactant. The increase of solution spray density will result in higher thermal resistance and the mass transfer coefficient decreases. In low solution spray density, the residence time of liquid film on tube surface is also relatively longer compared with high spray density, so the liquid film can absorb more vapor, and the best mass transfer performance is shown in $0.036 \text{ kg}/(\text{m}\cdot\text{s})$. As the spray density increases to $0.07 \text{ kg}/(\text{m}\cdot\text{s})$, the excess solution slide directly out of the tube and do not participate in the mass transfer process, so the change in the mass transfer coefficient is no longer significant.

As illustrated in Fig. 5, the mass transfer coefficient is improved significantly with the application of surfactant. The average mass transfer coefficient on the plain tube boosts by 450%, the floral tube boosts by 160% and the floral finned tube boosts by 60%. It is also seen that the mass transfer coefficients between the three tube types have been relatively close with the addition of surfactant. This is because the solution with surfactant has a strong Marangoni convection during the absorption process, which rises the mixing of solution. At the same time, the wetting properties of tube surface are greatly improved due to the decrease of surface tension. The results indicate that the effect of Marangoni convection is far greater than the tube surface structure. The mass transfer coefficient of floral tube is slightly higher than that of floral finned tube. This is because the fins may block the movement and mixing of liquid film on tube surface.

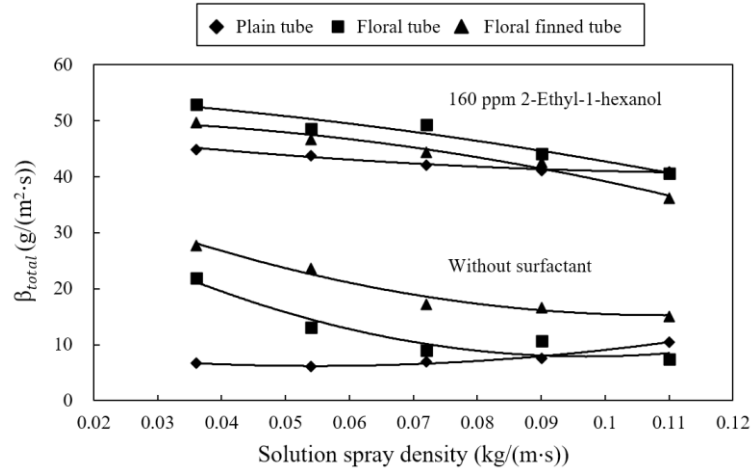


Fig. 5 Comparison of mass transfer coefficients on different tube types without and with 160 ppm 2-Ethyl-1-hexanol.

Fig. 6 shows the phenomenon of Marangoni convection during the liquid falling film absorption on the tube surface through sight glass. It can be seen from the figure that the solution is not evenly covered on the tube surface, and the falling film surface forms raised liquid rings. There is thin liquid film between the liquid rings which can wet the entire tube surface. This liquid film is not static, and there is strong disturbance and solution migration phenomenon. This unstable convection promotes the mixing of dilute solution on the surface and the solution inside the liquid film. Absorption heat can also be rapidly transmitted to the cooling water through this liquid film, so that the heat and mass transfer are significantly enhanced. It is the strong Marangoni convection that weakens the enhancement of tube surface structure.

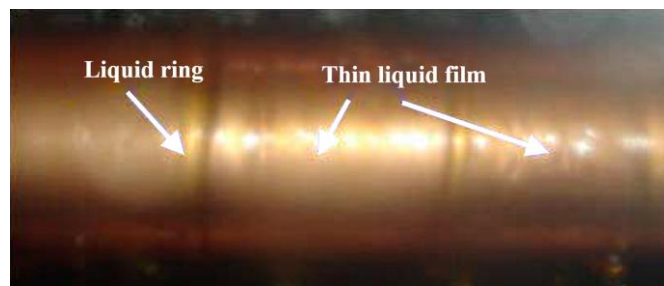


Fig. 6 Marangoni convection of the liquid film on tube surface during absorption

process.

Fig. 7 shows the heat transfer coefficient under different solution spray density on three tube types. The effects of flow rate, tube type and surfactant on the heat transfer coefficient are studied.

As shown in Fig. 7, the heat transfer coefficient rises as the spray density increases. Due to the increase of wetting rate, the heat exchange between the solution and the cooling water accelerates. The heat transfer coefficient of plain tube without surfactant is the highest, and it boosts rapidly with the increase of solution spray density. This is due to the coupling of heat and mass transfer to each other during the falling film absorption of horizontal tube bundle. Heat transfer and mass transfer are interrelated with each other. Compared with floral tube and floral finned tube, the liquid film on the plain tube surface absorbs less vapor, and the absorbed vapor releases less heat to the LiBr-H₂O solution while the heat transfer coefficient is larger. With the increase of flow rate, the wetted area of the plain tube rises, and the heat transfer coefficient boosts rapidly.

Compared with floral tube, using floral finned tube can absorb more vapor and release more absorption heat. However, the fins on the surface of the floral finned tube increase the disturbance of the solution and enhance the heat transfer, so the heat transfer coefficient of floral finned tube is higher than that of floral tube. Since the surface of enhancement tube (floral tube and floral finned tube) has good solution wetting characteristics, the change of heat transfer coefficient is not as obvious as that of the plain tube with the flow rate increases.

What's more, with the addition of surfactant, the Marangoni convection of liquid film on tube surface is the main factor for enhancing the heat transfer. The floral tube shows the highest mass transfer performance. The plain tube that absorbs the least vapor shows the highest heat transfer coefficient. Due to the influence of Marangoni convection, the heat transfer coefficient has a good performance under low solution flow rate. When the spray density increases gradually to 0.09 kg/(m·s), the heat transfer coefficient decreases. This is because when the flow rate exceeds the optimal value, the excess part of solution can no longer exchange heat with tube surface.

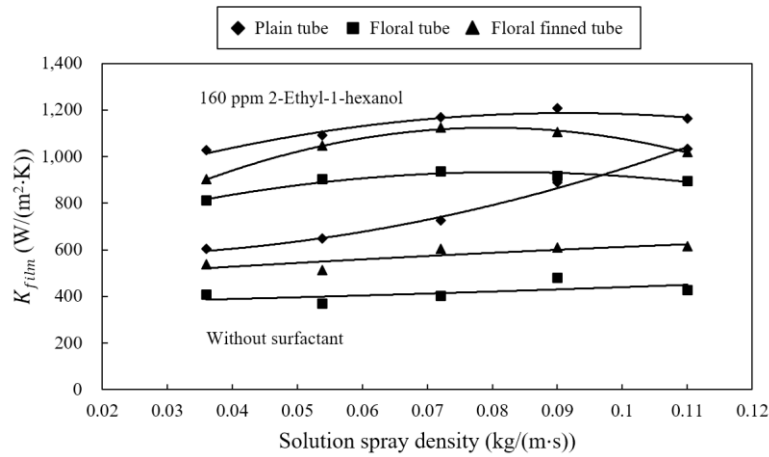


Fig. 7 Comparison of heat transfer coefficients on different tube types without and with 160 ppm 2-Ethyl-1-hexanol.

4.3 Effect of Surfactant Mass fraction on the Heat and Mass Transfer

Fig. 8 shows the heat and mass transfer enhancement factors for the 2-Ethyl-1-hexanol and 1-Octanol at the spray density of 0.09 kg/(m·s). The type of tube is plain tube. The enhancement factor is defined by the ratio of the heat and mass transfer coefficients at a certain surfactant mass fraction to that without surfactant.

As shown in Fig. 8, the enhancement factor gradually increases with the rise of 2-

Ethyl-1-hexanol mass fraction. The effect of surfactant on mass transfer is greater than that of heat transfer. The mass transfer coefficient increases from 220% to 400%, and the heat transfer coefficient increases from 120% to 200%. While the mass fraction of the surfactant reaches a certain value, the enhancement factor grows little. The results indicate that the heat and mass transfer coefficients reach the maximum value simultaneously when the surfactant mass fraction is about 80 ppm.

As to the 1-Octanol, it is seen that the enhancement factor of 1-Octanol is less than 2-Ethyl-1-hexanol. By using 1-Octanol as surfactant, the increase of heat transfer coefficients and mass transfer coefficients are from 105% to 170% and 150% to 350%, respectively. The optimal addition mass fraction of 1-Octanol is 160 ppm, which is different from 2-Ethyl-1-hexanol. It can be attributed to the effects of Marangoni convection. The Marangoni convection is caused by the imbalance of surface tension gradient of LiBr-H₂O solution. 2-Ethyl-1-hexanol can produce larger surface tension gradient and better effect of heat and mass transfer while the mass fraction is the same with 1-Octanol. When the mass fraction of surfactant is further increased, the surfactant floating on the solution surface forms diaphragm layer due to its lower solubility. It restrains the contact of vapor with LiBr-H₂O solution and reduces the vapor absorption, so the enhancement factor is slightly decreased.

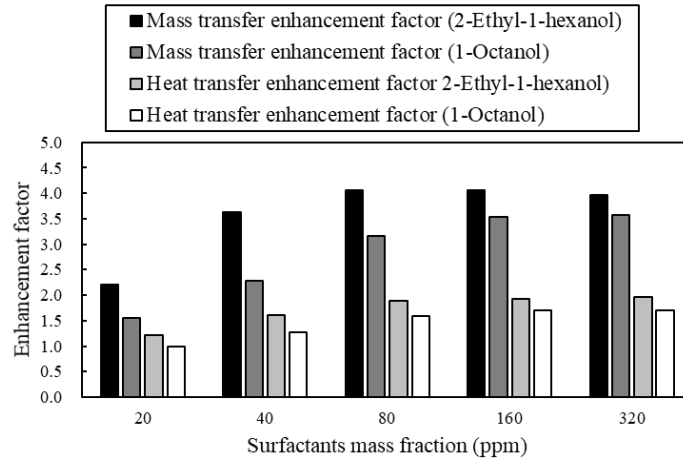


Fig. 8 Heat and mass transfer enhancement factors for different surfactants ($\Gamma = 0.09$

$\text{kg}/(\text{m}\cdot\text{s})$).

4.4 Influence of Spray Density on the Heat and Mass Transfer

Fig. 9 shows the variation of heat and mass transfer coefficients with different 1-Octanol mass fraction and spray density on plain tube. As illustrated in the figure, the heat and mass transfer coefficients boost rapidly with the increase of 1-Octanol mass fraction, and then they decrease slightly. This is because excessive surfactant floats on the surface of solution. This phenomenon increases thermal resistance and leads to poor heat transfer performance. It can be seen that the best mass fraction of surfactant is also increased with the rise of spray density. According to Kulankara's theory [18], the strength of Marangoni convection was determined by the mass fraction of surfactant on the surface of solution. As the spray density increases, it is difficult to transfer the surfactant from the inside of solution to the surface, so the best surfactant mass fraction is increased accordingly.

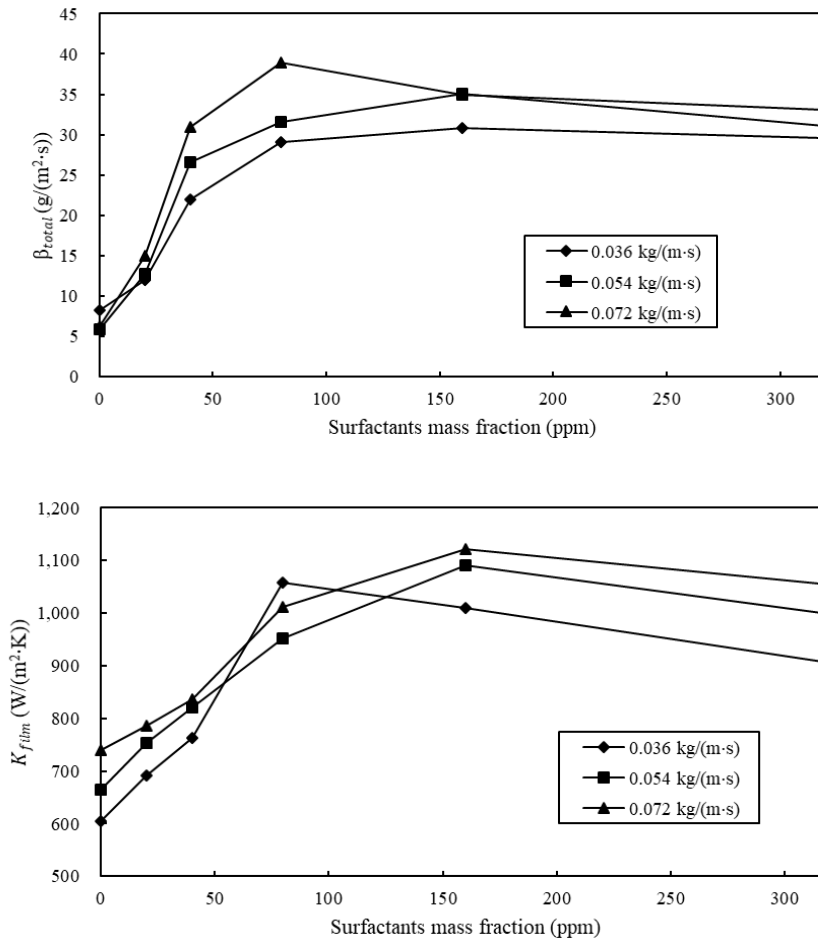


Fig. 9 Influence of spray density on the best mass fraction of surfactant (1-Octanol).

Comparisons of this study and Hoffmann's [7] are conducted with the application of 2-Ethyl-1-hexanol as surfactant, and the results are shown in Fig. 10. As illustrated in the figure, the deviation between this study and Hoffmann is small and the variation trend is similar. The Hoffmann's data is higher than that in this study at the initial stage, it can be attributed to the difference of tubes and tube surface roughness. With the same mass fraction of surfactant, the wetting rate of Hoffmann's tube is higher than that in this study even with the small spray density, so the heat transfer coefficient is higher. When the surfactant mass fraction is larger than 100 ppm, the results of these two studies are close to each other and the variation trends are very small. This is because

the tubes are completely wetted and the increase of surfactant can't affect the heat transfer performance when the surfactant mass fraction reaches 100 ppm. In the case that tubes are completely wetted, the effect of spray density is not obvious, so the heat transfer coefficient is close to each other. The results show that the test data in this paper are relatively reliable.

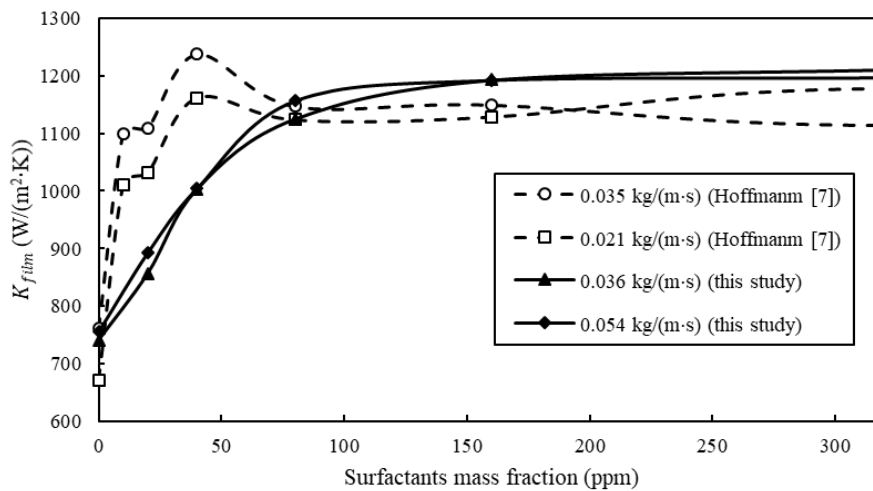


Fig. 10 Comparisons between this study and others. (2-Ethyl-1-hexanol)

5. Conclusion

An experimental setup for horizontal falling film absorber was designed and built to study the effects of two surfactants (2-Ethyl-1-hexanol and 1-Octanol) and three heat transfer tubes (plain tube, floral tube and floral finned tube). In this paper, a new enhanced tube (floral finned tube) is presented. Based on the previous research [7], the combined effects of tube type, surfactant and solution spray density are comprehensively analyzed. What's more, the influence of physical and operation parameters on the heat and mass transfer coefficients are also presented. The main conclusions of the present investigation can be summarized as:

1. The heat and mass transfer coefficients of each tube gradually decrease with

solution falling down on the tube bundles, and the heat and mass transfer coefficients of floral finned tube has the most stable variation trend on each row of tube bundles.

2. Due to the coupling effects of heat and mass transfer, the mass transfer coefficient of floral finned tube is the largest while the heat transfer coefficient is the smallest. At the same time, higher flow rates eventually lead to higher thermal resistances due to the increase in the film thickness, so that the mass transfer coefficient decreases. With the application of surfactant, the heat and mass transfer coefficients boost significantly, and the differences between the three tubes are reduced.

3. The effect of the surfactant on heat and mass transfer is obviously greater than that of tube surface geometry. 2-Ethyl-1-hexanol is superior to 1-Octanol in terms of heat and mass transfer enhancement. The surfactant has an optimum mass fraction range of 80-160 ppm for 2-Ethyl-1-hexanol and 160-320 ppm for 1-Octanol. As the solution flow rate increases, the optimal mass fraction of the surfactant grows.

4. The most stable and reliable combination of heat and mass transfer occurs in the condition of floral tubes with 2-Ethyl-1-hexanol, where the spray density is 0.03 - 0.06 kg/(m·s), and the solution mass fraction is 80 - 160 ppm.

References

[1] Rogdakis E, Papaefthimiou V, Karampinos D. A realistic approach to model LiBr-H₂O smooth falling film absorption on a vertical tube. *Applied Thermal Engineering*, 2003, 23(17): 2269-2283.

[2] Kyung I, Herold K, Kang Y. Model for absorption of water vapor into aqueous LiBr

flowing over a horizontal smooth tube. *International Journal of Refrigeration*, 2007, 30(4): 591-600.

[3] Zhao C, Ji W, He Y, Zhong Y, Tao W. A comprehensive numerical study on the subcooled falling film heat transfer on a horizontal smooth tube. *International Journal of Heat and Mass Transfer*, 2018, 119: 259-270.

[4] Triché D, Bonnot S, Perier-Muzet M, Boudéhenn F, Demasles H, Caney N. Experimental and numerical study of a falling film absorber in an ammonia-water absorption chiller. *International Journal of Heat & Mass Transfer*, 2017, 111:374-385.

[5] Álvarez M, Bourouis M. Experimental characterization of heat and mass transfer in a horizontal tube falling film absorber using aqueous (lithium, potassium, sodium) nitrate solution as a working pair. *Energy*, 2018, 148:876-887.

[6] Li T, Yin Y, Liang Z, Zhang X. Experimental study on heat and mass transfer performance of falling film absorption over a vertical tube using LiCl solution. *International Journal of Refrigeration*, 2018, 85:109-119.

[7] Hoffmann L, Greiter I, Wagner A, Weiss V, Alefeld G. Experimental investigation of heat transfer in a horizontal tube falling film absorber with aqueous solutions of LiBr with and without surfactants. *International Journal of Refrigeration*, 1996, 19(5): 331-341.

[8] Roques J, Dupont V. Falling Film Transitions on Plain and Enhanced Tubes. *Applied Thermal Engineering*, 2002, 124(3): 491-499.

[9] Kim H, Kang R. Effects of hydrophilic surface treatment on evaporation heat transfer at the outside wall of horizontal tubes, *Applied Thermal Engineering*. 2003, 23:

449-458.

[10] Zheng Y, Ma X, Li Y, Jiang R, Wang K, Lan Z, Liang Q. Experimental study of falling film evaporation heat transfer on superhydrophilic horizontal-tubes at low spray density. *Applied Thermal Engineering*, 2016, 111: 1548-1556.

[11] Arroiabe P, Martinez-Urrutia A, Peña X, Martinez-Agirre M, Bou-Ali M. Influence of the contact angle on the wettability of horizontal-tube falling films in the droplet and jet flow modes. *International Journal of Refrigeration*, 2018, 90:12-21.

[12] Lee S, Koroğlu B, Park C. Experimental investigation of capillary-assisted solution wetting and heat transfer using a micro-scale, porous-layer coating on horizontal-tube, falling-film heat exchanger. *International Journal of Refrigeration*, 2012, 35(4): 1176-1187.

[13] Ziegler F, Grossman G. Heat-transfer enhancement by additives. *International Journal of Refrigeration*, 1996, 19(5): 301-309.

[14] Yoon J, Kim E, Choi K, Seol W. Heat transfer enhancement with a surfactant on horizontal bundle tubes of an absorber. *International Journal of Heat and Mass Transfer*, 2002, 45(4): 735-741.

[15] Sun J, Zhang S. Experimental study on vertical vapor absorption into LiBr solution with and without additive. *Applied Thermal Engineering*, 2011, 31(14-15): 2850-2854.

[16] Kim D, Ferreira C. Flow patterns and heat and mass transfer coefficients of low Reynolds number falling film flows on vertical plates: Effects of a wire screen and an additive. *International Journal of Refrigeration*, 2009, 32(1): 138-149.

[17] Daiguji H, Hihara E, Saito T. Mechanism of absorption enhancement by surfactant.

International Journal of Heat and Mass Transfer, 1997, 40(40): 1743-1752.

[18] Kulankara S, Herold K. Surface tension of aqueous lithium bromide with heat/mass transfer enhancement additives: the effect of additive vapor transport. International Journal of Refrigeration, 2002, 25(3): 383-389.

[19] Giannetti N, Yamaguchi S, Saito K. Numerical simulation of Marangoni convection within absorptive aqueous Li-Br. International Journal of Refrigeration, 2018, 92:176-184.

[20] Miller W. The Synergism Between Heat and Mass Transfer Additive and Advanced Surfaces in Aqueous LiBr Horizontal Tube Absorbers. Office of Scientific and Technical Information Technical Reports, 1999.

[21] Francés V, Ojer J. Validation of a model for the absorption process of H₂O(vap) by a LiBr(aq) in a horizontal tube bundle, using a multi-factorial analysis. International Journal of Heat and Mass Transfer, 2003, 46(17):3299-3312.

[22] Deng S, Ma W. Experimental studies on the characteristics of an absorber using LiBr/H₂O solution as working fluid. International Journal of Refrigeration, 1999, 22(4):293-301.